Involvement of Phe[19] in the Mn^{2+}−L-Malate Binding and the Subunit Interactions of Pigeon Liver Malic Enzyme[†]

Wei-Yuan Chou,* Ming-Yuan Liu, Shih-Ming Huang, and Gu-Gang Chang

Department of Biochemistry, National Defense Medical Center, Taipei, Taiwan, Republic of China

Received January 26, 1996; Revised Manuscript Received May 16, 1996[⊗]

ABSTRACT: A triple mutant, F19S/N250S/L353Q, of pigeon liver malic enzyme was found to have no detectable enzymatic activity [Chou, W.-Y., Huang, S.-M., & Chang, G.-G. (1994) *Arch. Biochem. Biophys. 310*, 158−166]. In the present study, point mutants at these positions (F19S, N250S, and L353Q) were prepared by site-directed mutagenesis. Both N250S and L353Q have kinetic properties similar to those of the wild-type. On the other hand, the $K_{m(app)}$ values for both Mn^{2+} and L-malate of F19S were increased by approximately 10-fold, while the k_{cat} value was decreased by 5-fold, which results in a decrease of the apparent catalytic efficiency ($k_{cat}/K_{mNADP}K_{mMal}K_{mMn}$) by approximately 300-fold. These results clearly indicate that the F19S mutation is mainly responsible for the undetectable enzyme activity of the triple mutant. Three more Phe[19] mutants (F19Y, F19G, and F19A) were then prepared. There is a direct correlation between the size of the substitutes and the affinities for Mn^{2+} and L-malate. The kinetic parameters for F19Y were similar to those for wild-type. Both F19A and F19G reveal a 5-fold decrease of k_{cat} values. Two K_{dMn} values for the high- and low-affinity sites, respectively, were detectable for the wild-type. On the contrary, only one K_{dMn} value was detected for the F19 mutants, which was increased in the order of F19G > F19A > F19S > F19Y, with F19G being the most affected mutant. The K_{mMal} values of F19G and F19A were increased 100- and 6-fold, respectively. The catalytic efficiency ($k_{cat}/K_{mNADP}K_{dMal}K_{dMn}$) of F19G was decreased to only 0.01% of that of the wild-type. The above results clearly indicate that the hydrophobic aromatic ring at position 19 plays a critical role in L-malate and Mn^{2+} binding. Furthermore, all mutants that have a small residue at position 19 exist as monomers. Therefore, Phe[19] may locate in or near the regions for Mn^{2+}−L-malate binding as well as for the subunit contact. These results are compatible with the asymmetric model for the quaternary structure of malic enzyme we proposed previously [Chang, G.-G., Huang, T.-M., Huang, S.-M., & Chou, W.-Y. (1994) *Eur. J. Biochem. 225*, 1021−1027]. The possible roles of the N-terminus of malic enzyme were also addressed.

Cytosolic malic enzyme [(*S*)-malate:$NADP^+$ oxidoreductase (oxaloacetate-decarboxylating), EC 1.1.1.40] catalyzes the oxidative decarboxylation of L-malate to yield pyruvate and CO_2 with concomitant reduction of $NADP^+$ to NADPH. The generated NADPH is a source of the reducing equivalents necessary for the *de novo* biosynthesis of long-chain fatty acids (Frenkel, 1975). The enzyme from pigeon liver is a tetrameric protein composed of four chemically identical subunits with a molecular mass about 65 000 Da (Nevaldine *et al.*, 1974; Kam *et al.*, 1987). The enzyme was proposed to follow an ordered bi-ter kinetic mechanism with $NADP^+$ as the leading substrate followed by L-malate. The products are released in the order CO_2, pyruvate, and NADPH (Hsu *et al.*, 1967). The reaction follows a two-step mechanism with the hydride transfer preceding decarboxylation (Hermes *et al.*, 1982). On the basis of the chemical modification studies, histidine and lysine residues were proposed to be involved in the $NADP^+$ binding (Chang & Hsu, 1977b; Chang *et al.*, 1989). A tyrosine residue may be hydrogen bonded to C-4 of L-malate (Chang & Huang, 1980), and an arginine residue is ion paired with C-1 of L-malate (Chang & Huang, 1981). A carboxyl group from either the glutamate or the aspartate residue may serve as a general acid−base catalyst during the enzymatic reaction (Chang *et al.*, 1985). Since all these data were derived before the complete amino acid sequence was delineated, the exact positions of the these amino acid residues in the sequence are not known. By using affinity labeling and site-directed mutagenesis techniques, the nonessential residue Cys[99] was identified to be near the L-malate binding site (Satterlee & Hsu, 1991; Hsu *et al.*, 1992). More recently, we successfully utilize the metal-catalyzed oxidation systems and site-directed mutagenesis in identifying Asp[141], Asp[194], Asp[258], and Asp[464] as the coordinates for Mn^{2+} binding (Wei *et al.*, 1994, 1995; Chou *et al.*, 1995). Since X-ray crystallographic data are not available yet, the detailed structural requirements for substrate binding and catalysis are still unclear.

In our previous studies, we have isolated the full-length pigeon liver malic enzyme cDNA and successfully expressed it in *Escherichia coli* cells (Chou *et al.*, 1994). The steady-state kinetic properties of the recombinant wild-type enzyme were characterized, which were shown to be almost identical to those for the natural form. In that paper, we identified a triple mutant F19S/N250S/L353Q, which has no detectable enzymatic activity. None of these residues has been noticed to participate in substrate binding or catalysis in malic

[†] This work was supported by the National Science Council (Grant NSC84-2331-B016-063), Republic of China.

* To whom correspondence should be addressed: Department of Biochemistry, National Defense Medical Center, P.O. Box 90048-501, Taipei, Taiwan, Republic of China.

[⊗] Abstract published in *Advance ACS Abstracts,* July 1, 1996.

S0006-2960(96)00200-0 CCC: $12.00

Table 1: Synthetic Oligonucleotides for Site-Directed Mutagenesis of Pigeon Liver Malic Enzyme

mutant	synthetic oligonucleotides
N250S	5′-GCATAAGTACCGTAGCAAGTATTGC-3′
L353Q	5′-GAAATGAAAAATCAAGAAGATATTG-3′
F19S	5′-GGCATGGCTTCCACCTTGGAGG-3′
F19G	5′-AGGGCATGGCTGGCACCTTGGAGG-3′
F19A	5′-AAGGGCATGGCTGCTACCTTGGAGGAG-3′
F19Y	5′-GGCATGGCTTACACCTTGGAG-3′

enzyme. In this paper, we demonstrate that substitution of serine for phenylalanine at position 19 is responsible for the undetectable enzymatic activity of the triple mutant. Point mutations at Phe^{19} result in mutants with decreased affinities for L-malate and Mn^{2+}. Their k_{cat} values are also diminished. These point mutations also induce dissociation of the quaternary structure.

MATERIALS AND METHODS

Materials. Restriction endonucleases, T4 DNA polymerase, T4 DNA ligase, T4 polynucleotide kinase, and the TaqTrack sequencing system were purchased from Promega, Madison, WI. The [α-^{35}S]dATP (3000 Ci/mmol), [α-^{32}P]-dCTP (800 Ci/mmol), and the Sequenase kit were obtained from Amersham International, U.K. The pMAL-c2 expression vector was obtained from New England Biolabs, Beverly, MA. The pET-15b expression vector was purchased from Novagen, Madison, WI. Oligonucleotides were synthesized by Oligos Etc., Wilsonville, OR. All other reagents were of molecular biology grade. Natural pigeon liver malic enzyme was purified according to our published procedure (Chang & Chang, 1982).

Cloning of Pigeon Liver Malic Enzyme cDNA. Originally, we cloned the pigeon liver malic enzyme cDNA into the pET-15b vector for expression. However, it produced a low protein yield and lacked the M13 origin for single-strand DNA preparation. We thus shifted to the pMAL-c2 vector. Restriction endonuclease *Bam*HI-digested malic enzyme cDNA fragment was ligated with *Bam*HI- and *Xmn*I-double-digested pMAL-c2 vector through *Bam*HI sites. This linear DNA fragment, flanked with *Xmn*I and *Bam*HI, was blunt-ended with T4 DNA polymerase and then ligated to circular DNA. The directions of inserted malic enzyme cDNA were examined by restriction endonuclease digestion. The plasmid containing malic enzyme cDNA with corrected direction was named as pMAL-ME.

Site-Directed Mutagenesis. Site-directed mutagenesis of pigeon liver malic enzyme was carried out according to the procedures of Zoller and Smith (1982). Other DNA techniques were performed according to the protocols of Sambrook *et al.* (1989). The pMAL-ME plasmid was able to prepare single-strand DNA with helper phage due to the existence of the M13 origin. This recombinant phagemid was amplified in the *ung*$^-$ and *dut*$^-$ RZ1032 *E. coli* strain with helper phage R408 for preparation of the uracil-containing DNA template. The uracil-containing template DNA was annealed with phosphorylated mutagenic oligonucleotides (Table 1) and *in vitro* extended and ligated by T4 DNA polymerase and T4 DNA ligase, respectively. The mutated DNA was screened by transforming into the *ung*$^+$ and *dut*$^+$ JM109 *E. coli* strain, and the survival colonies were further identified by dideoxy chain termination sequencing (Sanger *et al.*, 1977). The entire cDNA was also sequenced to exclude any unexpected mutations resulting from *in vitro* DNA polymerase extension.

Expression and Purification of the Recombinant Pigeon Liver Malic Enzymes. In the pMAL-ME expression vector, the 5′ end malic enzyme cDNA was connected in-frame with maltose binding protein cDNA that facilitated the purification procedure of the expressed fusion protein by an amylose affinity column (New England Biolabs) (Guan *et al.*, 1987). This plasmid was transformed into TB1 bacteria. A 3 mL overnight culture from a single colony was grown in 80 mL of LB medium supplemented with 0.2% glucose and induced by 0.3 mM isopropyl β-D-thiogalactopyranoside (IPTG)[1] after the absorbance at wavelength 600 nm reached 0.5. The cells were harvested 4 h after IPTG induction. The cells were then sonicated in buffer A, which contains Tris-HCl buffer (25 mM, pH 7.5), NaCl (30 mM), and β-mercaptoethanol (2 mM). The recombinant proteins were purified with the amylose column according to the protocols supplied by the manufacturer. The fractions containing malic enzyme were further purified by an adenosine 2′,5′-bisphosphate agarose (Pharmacia-Biotech) column as follows. The column was washed with buffer A, but the concentration of NaCl was raised to 100 mM. The malic enzyme was then eluted by the same buffer containing 230 μM $NADP^+$.

Some of the mutants were unable to bind with the amylose column. In these cases, a Q-Sepharose (Pharmacia-Biotech) column was substituted for the amylose column according to the modified protocols for natural malic enzyme (Chang & Chang, 1982) in which the samples were washed and eluted by the buffer A containing 100 and 200 mM NaCl, successively. After purification, all samples were dialyzed exhaustively in buffer A (containing 10% glycerol) to remove $NADP^+$. All purified enzymes were subjected to sodium dodecyl sulfate−polyacrylamide gel electrophoresis (SDS−PAGE) to examine the purity and were typically about 95% pure. The protein concentrations were determined by the method of Bradford (1976) using purified pigeon liver malic enzyme as a standard.

Enzyme Assay and Kinetic Analysis. Malic enzyme activity was assayed according to Hsu and Lardy (1967). The reaction mixture contained triethanolamine hydrochloride buffer (66.7 mM, pH 7.4), L-malate (5 mM), $NADP^+$ (0.23 mM), Mn^{2+} (4 mM), and an appropriate amount of enzyme in a total volume of 1 mL. For some mutants, the concentrations of L-malate and Mn^{2+} were raised 10-fold to compromise the decrease in affinities for L-malate and Mn^{2+}. Since free Mn^{2+} and L-malate are the true reactants for malic enzyme, chelations due to formation of Mn^{2+}-L-malate and Mn^{2+}−$NADP^+$ complexes were corrected (Canellas & Wedding, 1980; Park *et al.*, 1984). The formation of NADPH at 30 °C was monitored continuously at 340 nm with a Perkin-Elmer Lambda 3B spectrophotometer. One unit of enzyme activity was defined as the initial rate of 1 μmol of NADPH formed per minute under the assay conditions. A molar absorption coefficient of 6.22×10^3 M^{-1} cm^{-1} for the NADPH was used in the calculations. Specific activity was defined as micromoles of NADPH formed per minute per milligram of protein.

Apparent Michaelis constants for the substrates were determined by varying one substrate concentration near the

[1] Abbreviations: IPTG, isopropyl β-D-thiogalactopyranoside; SDS, sodium dodecyl sulfate; PAGE, polyacrylamide gel electrophoresis.

K_m value and keeping the concentrations of the other components constant. The initial slopes of the recorder tracings were taken as initial velocities. To determine the true Michaelis and dissociation constants for Mn^{2+} and L-malate, an initial velocity study was performed, where both concentrations of Mn^{2+} and L-malate were varied. The experimental data were evaluated by EZ-FIT (Perrella, 1988), a curve-fitting microcomputer program using the Melder−Mead Simplex and Marquardt nonlinear regression algorithms sequentially.

Determination of Subunit Dissociation. The quaternary structure of the enzyme was examined by an 8 to 25% gradient PAGE under reducing conditions in the absence of SDS with a Pharmacia-Biotech PhastSystem according to our published procedure (Huang & Chang, 1992) with slight modifications. The proteins were not cross-linked with glutaraldehyde. Two gels were run in parallel; one of them was stained for protein with Coomassie Blue R-350 and the other stained for enzymatic activity. After electrophoresis and staining, the distribution of various enzyme forms was evaluated by scanning with a Molecular Dynamics computing laser densitometer and then quantified with the ImageQuant software. Enzyme activity staining was performed by immersing the gel into a solution containing triethanolamine hydrochloride buffer (55 mM, pH 7.4), $NADP^+$ (0.47 mM), L-malate (17.2 mM), $MnCl_2$ (2.75 mM), nitroblue tetrazolium (0.55 mg/mL), and phenazine methosulfate (0.097 mg/mL). After 2 h of incubation at room temperature, the reaction was stopped by replacing the staining solution with 5% acetic acid. The protein band with malic enzyme activity was stained a violet-blue color.

RESULTS

Expression and Purification of Recombinant Pigeon Liver Malic Enzyme and Its Mutants. In our early studies, the recombinant pigeon liver malic enzyme was expressed from the pET vector system, which contained a DNA sequence coding for a string of histidine. However, this system provides a low protein yield and lacks the ability to synthesize single-strand DNA for site-directed mutagenesis. We thus subcloned the malic enzyme cDNA into the pMAL-2c vector. This vector uses the maltose binding protein as a tag to facilitate the purification procedure and uses the strong P_{tac} promoter to express large amounts of fusion protein. However, the protein eluted from the amylose affinity column did not provide sufficient purity. A second affinity adenosine 2′,5′-bisphosphate agarose column was used to further purify the enzymes, which produced a single protein band on the SDS−PAGE gel for N250S, L353Q, and F19Y mutants.

The other three mutants, F19A, F19G, and F19S, were found to be unable to bind with the amylose column as tightly as wild-type protein (Table 2). A Q-Sepharose column was substituted in the purification of these mutants. These mutants also showed decreased affinities for the adenosine 2′,5′-bisphosphate agarose column. In order to get sufficient amounts of purified protein, we decreased the salt concentrations in both the binding and washing buffer, which increased the overall yield from 0.7 to 39%, and apparently, homogeneous proteins were still obtained as judged by SDS−PAGE (Figure 1A). All fusion proteins reveal M_r values corresponding to those of malic enzyme (M_r = 62 061) plus the maltose binding protein (M_r = 40 622).

Table 2: Purification of the Recombinant Wild-Type and F19A Mutant Malic Enzymes

purification step	total protein (mg)	total activity (U)[a]	specific activity (U/mg)	purification (-fold)	recovery (%)
wild-type	30.46	25.0	0.82	−	100
crude extract					
amylose column	0.92	16.8	18.4	22.4	67
2′,5′-ADP column	0.54	12.5	23.2	28.3	50
F19A					
protocol 1					
crude extract	23.5	14.9	0.6	−	100
amylose column	0.57	4.0	7.0	11.7	27
2′,5′-ADP column	0.004	0.1	0.7	1.2	0.7
protocol 2					
crude extract	19.75	10.2	0.5	−	100
Q-Sepharose	7.78	8.8	1.1	2.2	87
2′,5′-ADP column	0.44	4.0	9.1	18.2	39

[a] U is defined as micromoles of NADPH formed per minute under the assay conditions described in Materials and Methods.

Factor Xa Proteinase Digestion. In order to try to remove the fusing maltose binding protein, the wild-type and mutated malic enzyme fusion proteins were subjected to factor Xa digestion at 4 and 25 °C separately. Under these conditions, the fusion protein was successfully removed from F19A, F19G, and F19S recombinant proteins in 1 day. After digestion, the fusion proteins were cleaved into two fragments with M_r values corresponding to those of malic enzyme and the maltose binding protein (Figure 1B). However, the digestion was not successful for the wild-type fused protein. F19Y showed incomplete digestion under the same conditions. We did not try a higher temperature because factor Xa and malic enzyme may be unstable in the long course of digestion. In the presence of 0.1% SDS, the wild-type malic enzyme fusion protein was able to be cleaved completely, but the malic enzyme was denatured (data not shown). In comparison with our previous studies (Chou *et al.*, 1994), the steady-state kinetic parameters for the maltose binding protein-fused recombinant wild-type malic enzyme show no significant differences with respect to those of natural or His taq-connected malic enzyme. These results suggest that the fused moieties, either maltose binding protein or a string of histidine residues attached at the N-terminus, have no effect on the kinetic properties of malic enzyme. We thus used the fusion protein directly for further studies without factor Xa treatment. For the convenience of comparison, all mutant fusion proteins were also used directly.

Preliminary Kinetic Characterization of the Mutants. The purified recombinant wild-type malic enzyme showed a specific activity of 23.2 units/mg, which was comparable with that of natural pigeon liver malic enzyme (Hsu & Lardy, 1967). N250S and L353Q recombinant mutants were enzymatically active under the standard assay conditions. However, to detect the enzymatic activity for F19S, the Mn^{2+} and L-malate concentrations had to be raised at least 10-fold. The steady-state kinetic parameters of the wild-type and the three mutants of the pigeon malic enzyme are summarized in Table 3. All recombinant enzymes showed little but consistent change in K_{mNADP} (2-fold). It may result from a slight difference in the conformation of these mutants. The $K_{mMal(app)}$, $K_{mMn(app)}$, and k_{cat} values of N250S were almost identical to those of wild-type. L353Q shows only a 2-fold decrease in the value of k_{cat}. It may also result from a minor structural change in L353Q. However, F19S showed

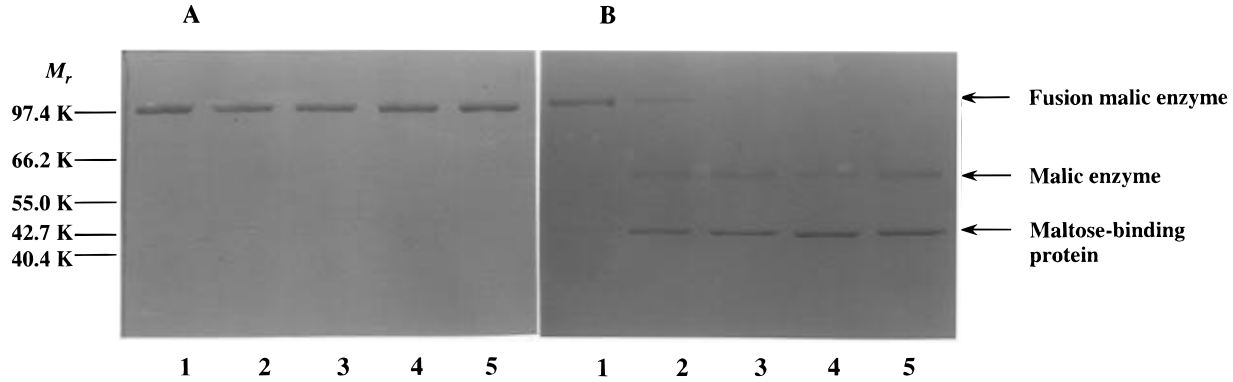

FIGURE 1: SDS-PAGE of the wild-type and various Phe[19] mutant pigeon liver malic enzymes. In panel A are malic enzymes fused with maltose binding protein. In panel B are the same protein samples which were digested by factor Xa at 25 °C for 24 h: lane 1, wild-type; lane 2, F19Y; lane 3, F19A; lane 4, F19G; and lane 5, F19S.

Table 3: Kinetic Parameters for the Wild-Type and Individual Point Mutants of the Triple Mutant F19S/N250S/L353Q

kinetic parameters	wild-type	F19S	N250S	L353Q
$K_{mMn(app)}$ (μM)	1.53 ± 0.06	14.67 ± 1.00	1.81 ± 0.14	1.47 ± 0.11
$K_{mMal(app)}$ (mM)	0.14 ± 0.00	1.58 ± 0.10	0.14 ± 0.01	0.15 ± 0.01
$K_{mNADP(app)}$ (μM)	13.45 ± 1.04	7.64 ± 0.47	7.38 ± 0.58	6.37 ± 0.22
k_{cat} (s^{-1})	223.8 ± 6.9	46.73 ± 2.84	202.3 ± 6.0	110.7 ± 1.7
$k_{cat}/K_{mMn}K_{mMal}K_{mNADP}$ (s^{-1} M^{-3})	7.77×10^{16}	2.64×10^{14}	10.8×10^{16}	7.88×10^{16}

pronounced changes in the $K_{mMal(app)}$, $K_{mMn(app)}$, and k_{cat} values. The apparent catalytic efficiency ($k_{cat}/K_{mNADP}K_{mMal}K_{mMn}$) of F19S was only 0.3% of that of the wild-type. These results clearly explain that the undetectable enzymatic activity of the triple mutant F19S/N250S/L353Q is due to the substitution of serine for phenylalanine at position 19.

We then constructed three mutants in which Phe[19] was replaced by glycine, alanine, and tyrosine, respectively. The kinetic parameters of these mutant enzymes were examined. The kinetic parameters for F19Y were found to be similar to those of wild-type. It indicates that the aromatic ring of the phenylalanine residue may play an important role in the Mn^{2+}−L-malate binding or catalysis. Indeed, removing this aromatic ring caused a prominent effect on k_{cat} and $K_{m(app)}$ values for Mn^{2+} and L-malate. Both F19A and F19G demonstrated a 5-fold decrease of k_{cat} values. Two $K_{mMn(app)}$ values corresponding to high- and low-affinity sites were detected for F19A but were increased by 90- and 10-fold, respectively. On the other hand, only one $K_{mMn(app)}$ value for the F19G mutant was detected, which was increased by 600-fold. The $K_{mMal(app)}$ values were also increased 50- and 2-fold for F19G and F19A, respectively (data not shown). To examine whether the changes in kinetic properties were due to the global structural changes in these F19 mutants, circular dichroism (CD) spectra of the wild-type and F19A, F19G, F19S, and F19Y mutant malic enzyme were determined. The CD spectra of the mutant proteins showed no significant differences with respect to those of wild-type recombinant protein (spectra available in the supporting information), indicating that no major structural changes had occurred as a result of these mutations.

Initial Velocity Studies of Phe[19] Mutants. The above experimental results clearly demonstrated the importance of Phe[19] in the Mn^{2+}-L-malate binding. We then performed the detailed initial velocity studies to evaluate the true Michaelis constants and dissociation constants for Mn^{2+} and L-malate. In order to determine both the tight and loose binding constants for Mn^{2+}, wide range concentrations were chosen to produce two well-separated linear regions, which were separately fitted to an equation describing the ordered bi-ter mechanism. For wild-type and all mutants, double-reciprocal plots with either Mn^{2+} or L-malate as the variable substrate were used, and series lines converging at or above the abscissa were obtained (figures available in the supporting information). These results showed that all mutants had a kinetic mechanism similar to that of the wild-type enzyme. F19Y and F19A seemed to possess two Mn^{2+} binding sites, and the two K_{mMn} values were closer than those for wild-type. It was difficult to obtain two well-separated linear segments in the double-reciprocal plot, and thus, only one K_{mMn} value presumably corresponding to the low-affinity site was obtained (Table 4). The Michaelis and dissociation constants for Mn^{2+} and L-malate were increased in all F19 mutants, with F19G being the most affected mutant. The effect of substitution on the kinetic parameters was in the order of F19G > F19A > F19S > F19Y. The catalytic efficiencies of F19S and F19G were only 0.1 and 0.01% of that of the wild-type. The above results clearly indicated the importance of the hydrophobic benzene ring in Phe[19] in the maintenance of the correct binding of L-malate and Mn^{2+}.

Quaternary Structure of the Cloned Malic Enzymes. Malic enzyme from pigeon liver is a tetrameric protein composed of identical subunits (Kam *et al.*, 1987). We have previously demonstrated that, under an acidic environment, the enzyme was reversibly dissociated to its constituted monomers (Chang *et al.*, 1988; Huang & Chang, 1992). The cloned malic enzyme with the fused histidine tag was also demonstrated to exist as tetramers at neutral or alkaline pH but dissociated at acidic pH (Chou *et al.*, 1994). However, when malic enzyme was fused with a maltose binding protein, it dissociated into dimers at neutral pH. Replacement of Phe[19] with less bulky amino acid residues further led the protein to dissociate into monomers (Figure 2). Both dimeric and monomeric enzymes were enzymatically active, in agreement with our previous results (Chang *et al.*, 1988, 1993, 1994; Huang & Chang, 1992).

Table 4: Kinetic Parameters for the Various F19 Mutants

kinetic parameters	wild-type	F19S	F19G	F19A	F19Y
K_{mMn} high affinity (μM)	0.42 ± 0.07				
K_{mMn} low affinity (μM)	4.13 ± 0.23	26.12 ± 2.16	22.56 ± 8.71	44.03 ± 2.57	8.49 ± 0.44
K_{dMn} high affinity (μM)	1.16 ± 0.32				
K_{dMn} low affinity (μM)	3.92 ± 0.41	49.85 ± 6.16	64.17 ± 8.50	60.05 ± 6.21	6.54 ± 0.89
K_{mMal} at low [Mn^{2+}] (mM)	0.15 ± 0.04				
K_{mMal} at high [Mn^{2+}] (mM)	0.18 ± 0.01	1.71 ± 0.12	19.64 ± 2.58	1.13 ± 0.04	0.28 ± 0.01
K_{dMal} at low [Mn^{2+}] (mM)	0.41 ± 0.08				
K_{dMal} at high [Mn^{2+}] (mM)	0.17 ± 0.02	3.26 ± 0.43	59.3 ± 25.3	1.54 ± 0.19	0.21 ± 0.03
$K_{mNADP(app)}$ (μM)	13.45 ± 1.04	7.64 ± 0.47	3.77 ± 0.18	3.80 ± 0.32	4.70 ± 0.19
k_{cat} (s^{-1})	223.8 ± 6.9	46.73 ± 2.84	45.99 ± 4.44	39.97 ± 2.51	207.8 ± 2.4
$k_{cat}/K_{dMn}K_{dMal}K_{mNADP}$ (s^{-1} M^3)	3.5×10^{16}	3.8×10^{13}	3.2×10^{12}	1.1×10^{14}	3.2×10^{16}

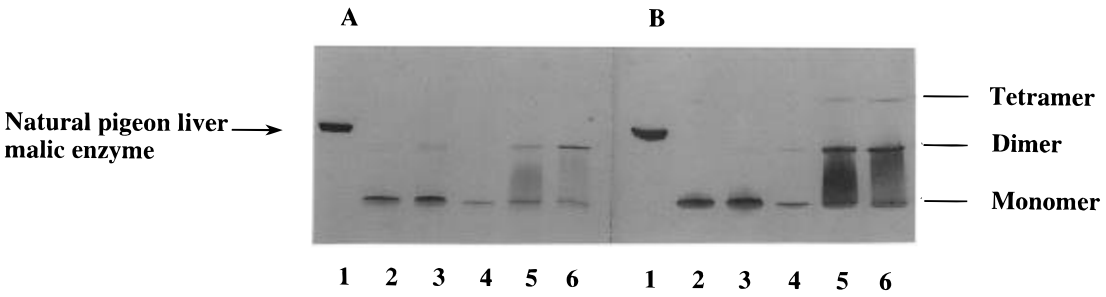

FIGURE 2: Polyacrylamide gel electrophoresis of wild-type and various Phe^{19} mutant malic enzymes under native conditions. Malic enzyme was subjected to 8 to 25% gradient polyacrylamide gel for 63 V/h. In panel A, the gel was stained by Coomassie blue. In panel B, the gel was stained for malic enzyme activity. For details of the activity stain, see Materials and Methods: lane 1, natural pigeon liver native enzyme; lane 2, F19A; lane 3, F19S; lane 4, F19G; lane 5, F19Y; and lane 6, wild-type. The molecular mass of the tetramer of natural pigeon liver malic enzyme is 248 244 Da (Chou *et al.*, 1994). It is 410 732 Da for the recombinant protein due to fusing with maltose binding protein (M_r = 40 622).

DISCUSSION

The experimental results presented in this paper clearly indicate that Phe^{19} is responsible for the diminished enzyme activity of the triple mutant F19S/N250S/L353Q. The essentialness of Phe^{19} was further explored by point mutation at Phe^{19}. Substitution of tyrosine for phenylalanine makes no difference in kinetic parameters, indicating the importance of the aromatic benzene ring for the enzyme activity. It also indicates that the kinetic differences for F19S may not result from the hydroxyl group of the serine residue. The F19A, which has a methyl side chain, showed a moderate change in the kinetic parameters. When phenylalaine was replaced by glycine, the most dramatic changes in the kinetic parameters were observed. We have also constructed a leucine mutant with a relatively bulky group, but expression of the recombinant protein was unsuccessful for unknown reasons (data not shown). It might be due to the instability of F19L in the *E. coli* system. These results imply that Phe^{19} plays an important role in the maintenance of the proper protein structure due to its hydrophobic character.

The importance of the aromatic ring in the active center of some enzymes has been noticed. In some studies, the aromatic ring was proposed to directly participate in catalysis. For example, in the active site of 3-oxo-Δ^5-steroid isomerase, Phe^{101} has been demonstrated to be important in proton transfer by stabilizing the intermediate dienolate and the transition states (Brothers *et al.*, 1995). Replacement of Phe^{101} by nonaromatic residues decreases the k_{cat} value but has little effect on the K_m of the substrate. Phe^{34} of human dihydrofolate reductase was also found to play critical roles in substrate and inhibitor binding and in catalysis (Nakano *et al.*, 1994). Replacement of Phe^{34} with smaller residues decreased affinities for methotrexate and also lowered the catalytic efficiencies. In our studies, we demonstrate that substitution of Phe^{19} by the nonaromatic residues in pigeon liver malic enzyme causes reduction of not only the k_{cat} value but also the Mn^{2+} and L-malate binding affinities. Inasmuch as the three-dimensional structure of the enzyme has not yet been determined, it is premature to predict the precise role of Phe^{19} in the active center. However, several laboratory observations should be able to give us some notions for the role of Phe^{19}. We have identified Asp^{258}, Asp^{141}, Asp^{194}, and Asp^{464} as the metal coordinates for malic enzyme (Wei *et al.*, 1994, 1995; Chou *et al.*, 1995). Since Mn^{2+} chelating required ionic bonds, Phe^{19} may not be directly involved as the Mn^{2+} ligand. On the contrary, Phe^{19} may interact with Mn^{2+} by hydrophobic interaction. Yamashita *et al.* (1990) have noticed that metal ions appear to bind in regions of proteins with high amphiphilic contrast in which the metal site is centered in a hydrophobic shell. Phe^{19} may play an important role in forming such a shell. The binding of Mn^{2+} at the hydrophobic shell has the advantage in that it restricts the flexibility of the site, and the low dielectric of the hydrophobic sphere enhances electrostatic interactions between groups within it (Regan, 1993).

The hydrophobic amino acid residue may also participate in the substrate binding through van der Waals interaction. For example, the maltose binding protein was shown to have hydrogen bonding as well as van der Waals interactions derived from four aromatic residues as revealed by X-ray crystallographic studies on the maltose binding (Spurlino *et al.*, 1991). In our previous studies, a truncated malic enzyme lacking the first 14 amino acid residues was found to be void of enzyme activity (Chou *et al.*, 1994). It is possible that the diminished enzyme activity of these two proteins results from the same cause. Since the truncated protein still has Phe^{19}, Phe^{19} may not contribute direct effects on binding and catalysis. The Phe^{19} of malic enzyme should be in a position

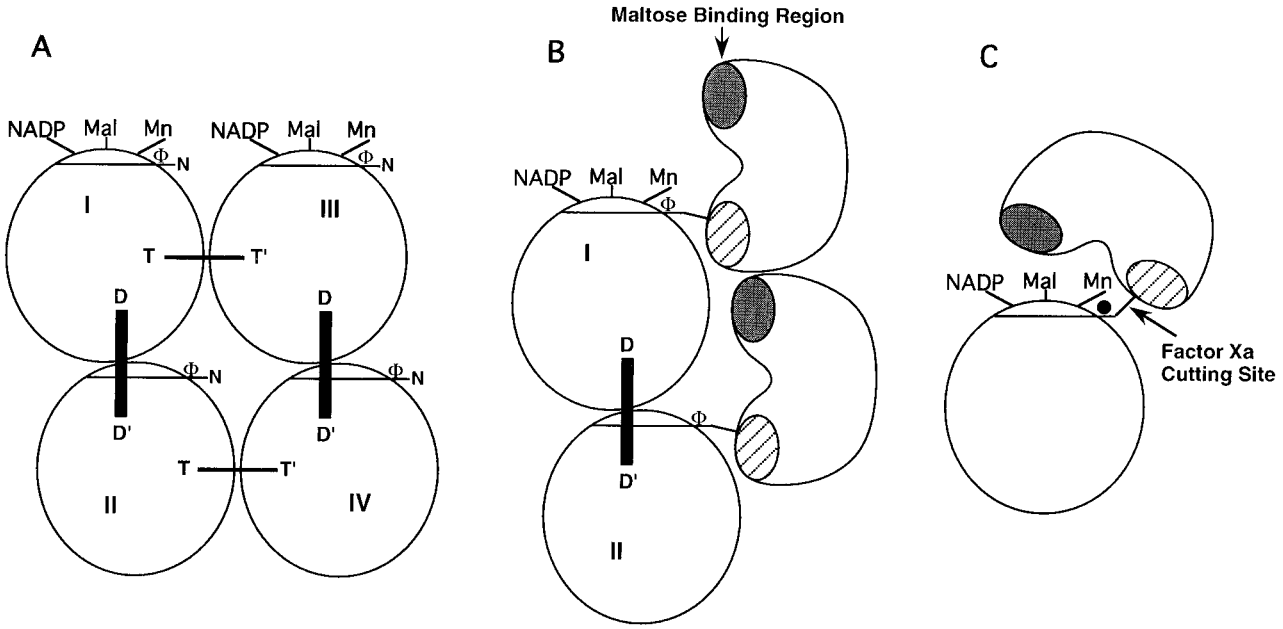

FIGURE 3: Schematic models for the quaternary structure of natural and recombinant pigeon liver malic enzyme. (A) Natural malic enzyme is shown as an asymmetric model as we proposed previously to account for the half-of-the-sites reactivity of the enzyme. D−D′ denotes the head-to-tail interactions, which are stronger than the T−T′ interactions. The N-terminus is shown in the active-site region, at the top of each monomer. Φ denotes the aromatic amino acid Phe or Tyr at position 19, while nonaromatic substitution (Ala, Ser, or Gly) is represented by a dot (●). (B) Dimeric recombinant wild-type malic enzyme or the F19Y mutant fused with a maltose binding protein. The maltose binding region is represented by the gray area, and the factor Xa cutting region is represented by the hatched area. (C) Monomeric F19S, F19A, or F19G mutants showing masking of the maltose binding domain but exposure of the factor Xa cutting region (see text for details). Both D−D′ and T−T′ interactions are disturbed.

that is in or near the active site affecting the alignment of other residues for both L-malate and Mn^{2+} binding. It also suggested that the N-terminus, the first 14 amino acid residues, must contain some key factors for binding and catalysis. Several charged amino acids in the N-terminus may be good candidates for exploring the direct substrate binding ligands.

During the purification stage of the mutant proteins, all mutants that showed altered kinetic parameters and quaternary structure also changed in affinities for both amylose and adenosine 2′,5′-bisphosphate agarose affinity columns. However, we observed no significant difference in K_{mNADP} values for all mutants as compared to that of wild-type. In our previous studies, adenosine 2′,5′-bisphosphate was found to be the essential fragment for $NADP^+$ binding (Lee & Chang, 1987). These results suggest that the conformation of the mutants in their $NADP^+$ binding site is intact; the altered binding affinity of some mutants with the adenosine 2′,5′-bisphosphate agarose column must be due to steric hindrance from fused maltose binding protein, which causes the enzyme to be inaccessible to adenosine 2′,5′-bisphosphate that is immobilized on agarose beads, but is still accessible to free $NADP^+$. Some of the mutant malic enzymes were unable to bind efficiently with the amylose column. It could also result from steric hindrance.

To explain these phenomena explicitly, we propose a working model for the quaternary structure of these recombinant malic enzymes as shown in Figure 3. The wild-type malic enzyme is presented as an asymmetric double dimer to account for the various kinetic and dissociation observations (A in Figure 3) (Hsu *et al.*, 1976; Chang & Hsu, 1977a; Dalziel *et al.*, 1983; Chang *et al.*, 1988, 1993, 1994; Lee & Chang, 1990; Huang & Chang, 1992). We propose that Phe^{19} is located in a region which connects malic enzyme and the maltose binding protein. In this region, the aromatic ring of Phe^{19} is located at such a position that it can uphold the maltose binding protein away from the malic enzyme active site but interferes with the T−T′ interactions (B in Figure 3). Therefore, the enzymatic activity of the wild-type recombinant enzyme is not influenced by the fusion protein, but the protein exists as dimers. The benzene ring of Phe^{19} may be directly involved in the subunit interaction through hydrophobic interactions. Alternatively, replacement of Phe^{19} may result in changing the local conformation, which is essential for the subunit association. The maltose binding ability of the recombinant wild-type enzyme is retained because the maltose binding region of the fusion protein is exposed.

This model can also explain the different specificities in factor Xa digestion of the fusion malic enzyme. The cleavage site in the fusion wild-type protein is located in such a position that it is masked from factor Xa attack. When the phenylalanine is replaced by other amino acid residues that have no aromatic ring, the N-terminus of the enzyme would bring these two protein moieties close to each other, making the protein inaccessible to their cognate affinity columns. Movement of the fusion protein in F19S, F19A, or F19G mutants produces more complex protein−protein interactions. It may change the environment of the cleavage site which then becomes accessible to factor Xa. Both the D−D′ and T−T′ interactions are disturbed. The F19S, F19A, or F19G mutants thus exist primarily as monomers. This possibility suggests that mutation at Phe^{19} on the malic enzyme alone may not cause such dramatic changes in kinetic parameters and subunit association. However, the fused maltose binding protein augments the effects on the conformation of the active center and subunit interactions.

This model is also in accordance with the possible involvement of the N-terminus of malic enzyme in enzymatic

reaction. It implies that the geometry of the N-terminus may be determined by the phenyl group of Phe^{19}, which is a hinge. The aromatic ring is essential to keep the flanking region in a correct geometry for the active center. Replacement of this aromatic residue with any less bulky group may place the N-terminus in an improper conformation, resulting in an increase in K_m for the substrate and a decrease in k_{cat}.

Pigeon liver malic enzyme reversibly dissociates under an acidic environment in the sequence of tetramer−dimer−monomer. At any intermediate pH value between 4.5 and 8.0, the enzyme exists as a mixture of three forms (Chang *et al.*, 1988). In our previous studies, we were able to immobilize monomeric malic enzyme on the Sepharose beads (Chang *et al.*, 1993). The apparent Michaelis constants for L-malate, Mn^{2+}, and $NADP^+$ of the immobilized monomers were similar to those of immobilized tetramers. In the present study, the enzyme is similarly immobilized on a maltose binding protein. However, we observed different kinetic properties between the dimeric wild-type and the monomeric mutants. This suggests that the differences are not due to subunit dissociation; instead, it really reflects the characters of the mutation itself. The significance of the present work is twofold. First, we have characterized the possible role of Phe^{19} of the enzyme. Second, for the first time, we are able to construct a dimeric pigeon enzyme. It provides a useful tool to evaluate our asymmetric model for the enzyme.

In conclusion, our results indicate that mutation at Phe^{19} of pigeon malic enzyme fusion protein affects both enzyme kinetic behavior and subunit interactions. Phe^{19} may not directly participate in Mn^{2+}−L-malate binding or catalytic reaction but may be located in or near the active site region, which also involves it in the subunit interaction. It also implies that the N-terminus of malic enzyme may play an important role in both properties.

SUPPORTING INFORMATION AVAILABLE

CD spectra and double-reciprocal plots of initial velocity studies of Phe^{19} mutants (3 pages). Ordering information is given on any current masthead page.

REFERENCES

Bradford, M. M. (1976) *Anal. Biochem. 72*, 248−254.

Brothers, P. N., Blotny, G., Qi, L., & Pollack, R. M. (1995) *Biochemistry 34*, 15453−15458.

Canellas, P. F., & Wedding, R. T. (1980) *Arch. Biochem. Biophys. 199*, 259−264.

Chang, G.-G., & Hsu, R. Y. (1977a) *Biochemistry 16*, 311−320.

Chang, G.-G., & Hsu, R. Y. (1977b) *Biochim. Biophys. Acta 483*, 228−235.

Chang, G.-G., & Huang, T.-M. (1980) *Biochim. Biophys. Acta 611*, 217−226.

Chang, G.-G., & Huang, T.-M. (1981) *Biochim. Biophys. Acta 660*, 341−347.

Chang, G.-G., Huang, T.-M., & Wuu, J. A. (1985) *Proc. Natl. Sci. Counc., Repub. China, Part B: Life Sci. 9*, 56−66.

Chang, G.-G., Huang, T.-M., & Chang, T.-C. (1988) *Biochem. J. 254*, 123−130.

Chang, G.-G., Shiao, M.-S., Liaw, J.-G., & Lee, H.-J. (1989) *J. Biol. Chem. 264*, 280−287.

Chang, G.-G., Huang, T.-M., & Chang, T.-C. (1993) *Eur. J. Biochem. 213*, 1159−1165.

Chang, G.-G., Huang, T.-M., Huang, S.-M., & Chou, W.-Y. (1994) *Eur. J. Biochem. 225*, 1021−1027.

Chang, J.-T., & Chang, G.-G. (1982) *Anal. Biochem. 121*, 366−369.

Chou, W.-Y., Huang, S.-M., Liu, Y.-H., & Chang, G.-G. (1994) *Arch. Biochem. Biophys. 310*, 158−166.

Chou, W.-Y., Tsai, W.-P., Lin, C.-C., & Chang, G.-G. (1995) *J. Biol. Chem. 270*, 25935−25941.

Dalziel, K., Hsu, R. Y., Matthews, B., & Soulie, J. M. (1983) *Biochemistry 22*, 5359−5365.

Frenkel, R. (1975) *Curr. Top. Cell. Regul. 9*, 157−181.

Guan, C., Li, P., Riggs, P. D., & Inouye, H. (1987) *Gene 67*, 21−30.

Hermes, J. D., Roeske, C. A., O'Leary, M. H., & Cleland, W. W. (1982) *Biochemistry 21*, 5106−5114.

Hsu, R. Y., & Lardy, H. A. (1967) *J. Biol. Chem. 242*, 520−526.

Hsu, R. Y., Lardy, H. A., & Cleland, W. W. (1967) *J. Biol. Chem. 242*, 5315−5322.

Hsu, R. Y., Mildvan, A. S., Chang, G.-G., & Fung, C.-H. (1976) *J. Biol. Chem. 251*, 6574−6583.

Hsu, R. Y., Glynias, M. J., Satterlee, J., Feeney, R., Clarke, A. R., Emery, D. C., Roe, B. A., Wilson, R. K., Goodridge, A. G., & Holbrook, J. J. (1992) *Biochem. J. 284*, 869−876.

Huang, T.-M., & Chang, G.-G. (1992) *Biochemistry 31*, 12658−12664.

Kam, P. L., Lin, C. C., & Chang, G.-G. (1987) *Int. J. Pept. Protein Res. 30*, 217−221.

Lee, H.-J., & Chang, G.-G. (1987) *Biochem. J. 245*, 407−414.

Lee, H.-J., & Chang, G.-G. (1990) *FEBS Lett. 277*, 175−179.

Nakano, T., Spencer, H. T., Appleman, J. R., & Blakley, R. L. (1994) *Biochemistry 33*, 9945−9952.

Nevaldine, B. H., Bassel, A. R., & Hsu, R. Y. (1974) *Biochim. Biophys. Acta 336*, 283−293.

Park, S. H., Kiick, D. M., Harris, B. G., & Cook, P. F. (1984) *Biochemistry 23*, 5446−5453.

Perrella, F. W. (1988) *Anal. Biochem. 174*, 437−447.

Regan, L. (1993) *Annu. Rev. Biophys. Biomol. Struct. 22*, 257−287.

Sambrook, J., Fritsch, E. F., & Maniatis, T. (1989) *Molecular Cloning: A Laboratory Manual*, 2nd ed., Cold Spring Harbor Laboratory Press, Plainview, NY.

Sanger, F., Nicklen, D., & Coulson, A. R. (1977) *Proc. Natl. Acad. Sci. U.S.A. 74*, 5463−5467.

Satterlee, J., & Hsu, R. Y. (1991) *Biochim. Biophys. Acta 1079*, 247−252.

Spurlino, J. C., Lu, G.-Y., & Quiocho, F. A. (1991) *J. Biol. Chem. 266*, 5202−5219.

Wei, C.-H., Chou, W.-Y., Huang, S.-M., Lin, C.-C., & Chang, G.-G. (1994) *Biochemistry 33*, 7931−7936.

Wei, C.-H., Chou, W.-Y., & Chang, G.-G. (1995) *Biochemistry 34*, 7949−7954.

Yamashita, M. M., Wesson, L., Eisenman, G., & Eisenberg, D. (1990) *Proc. Natl. Acad. Sci. U.S.A. 87*, 5648−5652.

Zoller, M. J., & Smith, M. (1982) *Nucleic Acids Res. 10*, 6487−6500.

BI960200G